

Supporting Information

Title: Adsorptive Catalysis of Hierarchical Porous Heteroatoms-Doped Biomass: From Recovered Heavy Metal to Efficient Pollutant Decontamination

Jing Wang,^a Qingfeng Yang,^a Weixia Yang,^a Hanna Pei,^a Liang Zhang,^a Tianshu Zhang,^a Na Hu,^b Yourui Suo,^b Jianlong Wang ^{a*}

^a College of Food Science and Engineering, Northwest A&F University, Yangling, 712100, Shaanxi, China.

^b Northwest Institute of Plateau Biology, Chinese Academy of Sciences, Xining, 810008, Qinghai, P. R. China.

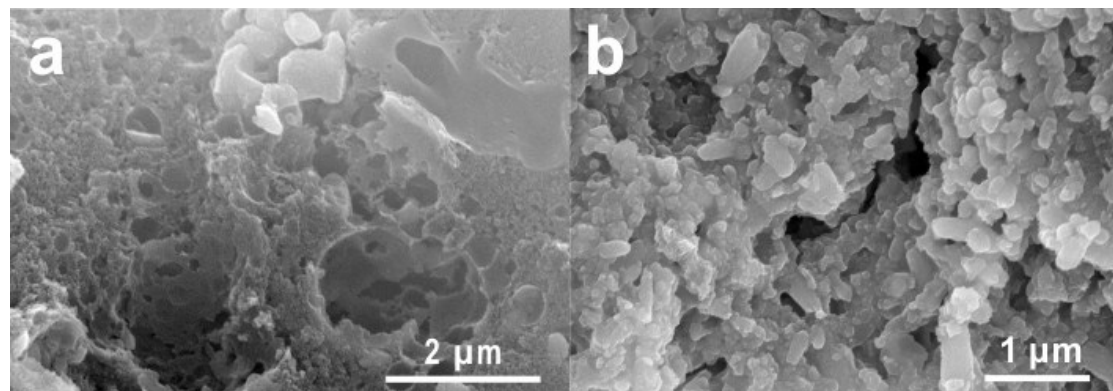


Figure S1. SEM image of the prepared a) CK and b) CS.

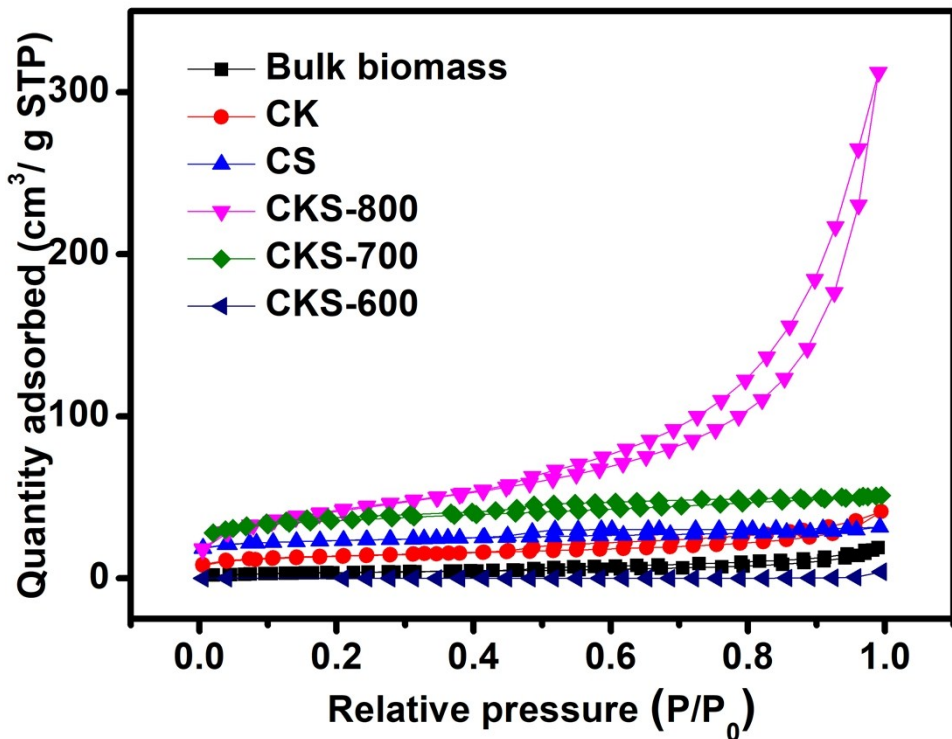


Figure S2. N₂ sorption isotherms of different biomass composites.

Table S1. Physico-chemical properties of the hierarchical porous carbons.

materials	textural properties			element composition (wt %)			
	S _{BET} (m ² g ⁻¹)	pore volume	pore size distribution	C	N	O	S
		(cm ³ g ⁻¹)	(nm)				
Bulk biomass	12.62	0.031	1.152	63.43	1.53	27.46	-
CK	47.78	0.062	5.15	64.15	1.68	26.03	-
CS	79.77	0.049	2.44	66.97	1.72	12.65	5.04
CKS-600	66.49	0.059	4.08	63.44	2.62	12.17	4.62
CKS-700	111.76	0.079	2.83	72.11	1.17	8.52	7.13
CKS-800	152.08	0.481	12.54	78.18	1.05	5.89	9.42
CKS-Cu	154.64	0.431	11.37	-	-	-	-
Regenerated							
CKS	137.47	0.293	8.36	-	-	-	-
CKS-Cu after	147.15	0.395	8.23	-	-	-	-

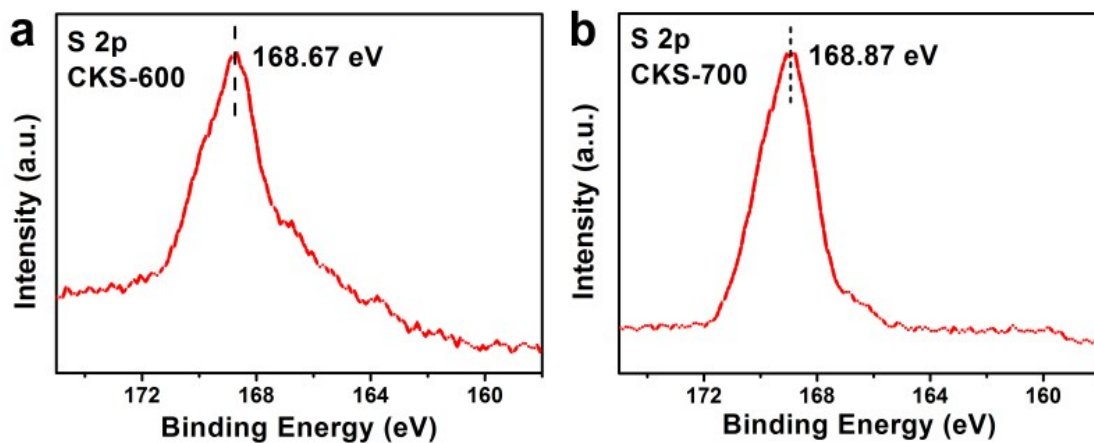


Figure S3. XPS spectra S 2p signal deconvolution of CKS-600 and CKS-700.

Results

	Mean (mV)	Area (%)	St Dev (mV)
Zeta Potential (mV): 8.24	Peak 1: 8.24	100.0	3.87
Zeta Deviation (mV): 3.87	Peak 2: 0.00	0.0	0.00
Conductivity (mS/cm): 1.35	Peak 3: 0.00	0.0	0.00

Result quality Good

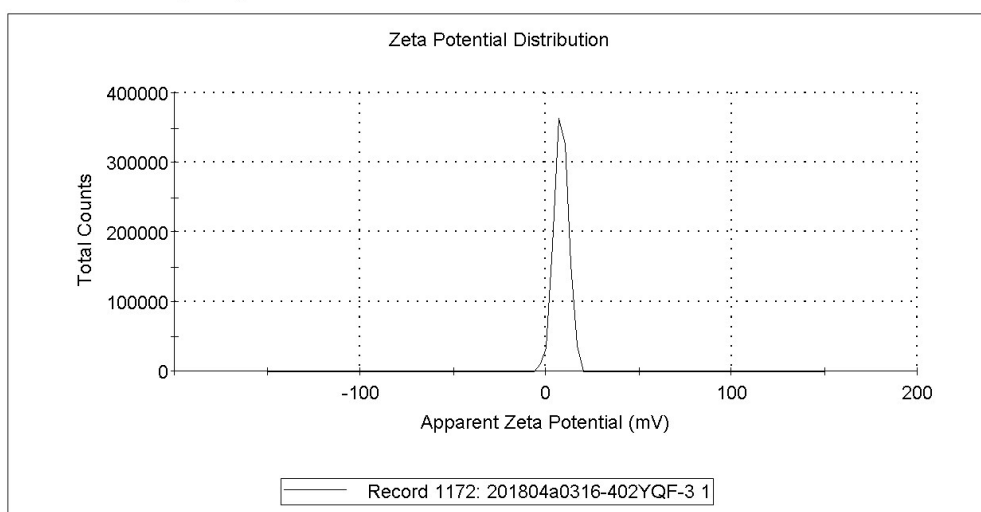


Figure S4. Zeta potential of hierarchical porous CKS biomass.

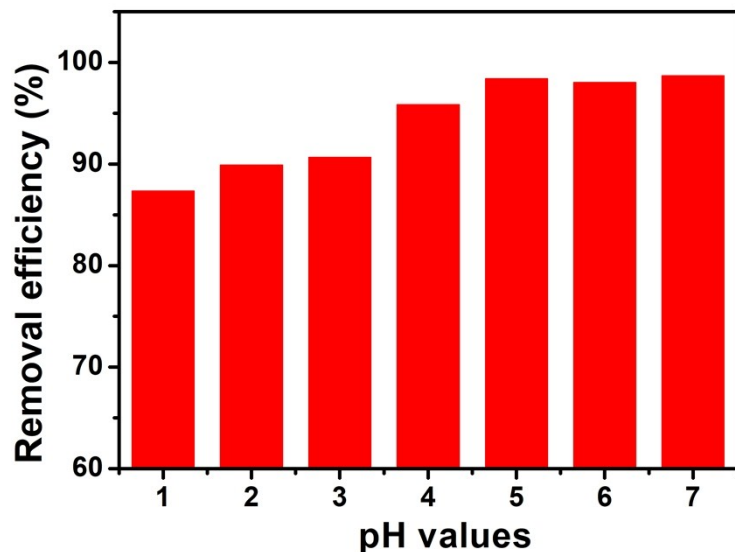


Figure S5. Removal efficiency of CKS toward Cu(II) under different pH values.

Table S2. Initial (before adsorption) and final (after adsorption) pH values

	pH values					
initial	1.21	2.32	3.07	4.01	5.20	6.14
final	1.18	2.24	2.94	3.89	5.01	5.87

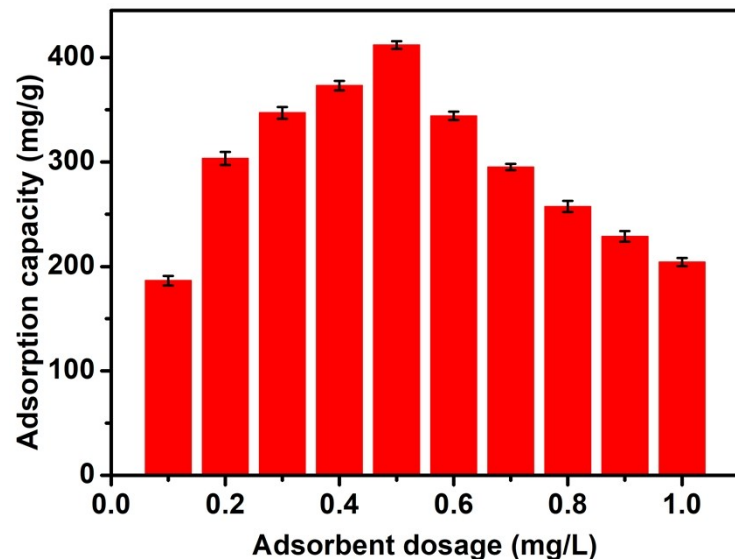


Figure S6. Adsorption capacities of CKS toward 300 ppm of Cu(II) under different adsorbent dosage.

Table S3. Kinetic parameters of metal ions adsorption on CKS

Single ions	pesudo-second-order				
	q_e , exp (mg/g)	k_2 (g/mg min)	q_e , cal (mg/g)	R^2	Fitting equation
Cu ²⁺	412.10	0.0002	414.14	0.997	$t/q=0.029+0.002t$
Ni ²⁺	312.88	0.0009	322.58	0.996	$t/q=0.011+0.003t$
Pb ²⁺	267.53	0.0003	264.12	0.998	$t/q=0.047+0.004t$

Table S4. Isotherm parameters of metal ions adsorption on CKS

sing le ions	$q_{m,exp}$ (mg/g)	Langmuir isotherm model			Freundlich isotherm model			
		k_L	q_m , cal (mg/g)	R^2	Fitting equation	K_F (mg/g)	n	R^2
Cu ²⁺	1356.62	0.0071	1366.67	0.991	$C_e/q_e=0.1+0.0007C_e$	110.58	2.4888	0.9209
Ni ²⁺	1122.63	0.0104	1250.21	0.994	$C_e/q_e=0.08+0.0008C_e$	228.40	4.0766	0.9432
Pb ²⁺	612.31	0.0072	619.23	0.996	$C_e/q_e=0.22+0.0016C_e$	65.75	2.8353	0.9723

Table S5. XPS analysis of Surface Functionality

content/functionality (at.%)	CKS	CKS-Pb	CKS-Cu
total oxygen content	43.02	19.58	15.37
total sulfur content	10.73	1.63	1.41
O-M	7.18	9.02	9.17
O=C-O	4.45	3.82	2.38

Table S6. Estimated total cost for preparing 1 g of nanoadsorbents and corresponding adsorption capacities.

classification	adsorbent	material	amount used	unit cost (dollar)	Cost (dollar)	total cost (dollar)	Cu ²⁺ adsorption capacity	k ₂ (g/mg min)	ref
	Hematite ($\alpha\text{-Fe}_2\text{O}_3$)	FeCl ₃	2.7	6.52	17.60	21.75	84.46	0.0025 ($C_{\text{Cu}^{2+}, \text{initial}} = 3.79 \text{ mg L}^{-1}$)	1
		DI water	500	0.0226	11.3				
		HCl	0.05	0.549	0.027				
	$\gamma\text{-Fe}_2\text{O}_3$	DI water	200	0.0226	4.52	19.01	26.8	-	2
		FeCl ₃	5.2	6.52	33.90				
		FeCl ₂	2	3.18	6.36				
		NH ₄ OH	1.5	0.0826	0.1239				
		Tetramethylammonium hydroxide	1	0.2264	0.2264				
		99% Octyl ether	N/A	N/A					
metal oxide-based		NaSO ₄	0.15 M, 250 mL	0.1042	0.56				
nanoadsorbent	$\alpha\text{-MnO}_2$ (OMS-1)	MnSO ₄	$C_{\text{Mn}^{2+}}=0.6 \text{ M}, 400 \text{ mL}$	0.273	11.07	1.84	57.6	-	3
		NaOH	5 M, 400 mL	0.1886	15.09				
		MgCl ₂	1M	0.537	12.24				
$\alpha\text{-MnO}_2$ (OMS-2)		DI water	250	0.0226	5.65	10.35	83.2	-	4
		65% HNO ₃	11.5	0.41	2.46				
		KMnO ₄	2.1	1.592	3.34				
TiO ₂ monolith		TiO ₂	4.6	8.68	39.93	18.68	398.72	-	5
		HCl	1M, 1000	0.046	46				
		5 M, tetrabutylammonium	N/A	8.08	N/A				
carbohydrate	TEMPO	CNC	1 g	0.3	0.3	2.72	268.2	-	6

		oxided CNC							
		TEMPO	0.059	0.57	0.33				
		NaBr	0.325 g	0.112	0.04				
		NaClO	7.1 mL	0.19	1.35				
		Methanol	11 mL	0.063	0.7				
		NaOH	N/A	0.008	N/A				
		HCl	N/A	0.01	N/A				
based-adsorbent	Succinic anhydride/CN C	CNC	1 g	0.3	0.3	0.78	121.6	-	6
	Succinic anhydride		0.6 g	0.26	0.16				
	Sodium hydrogenc arbonate		N/A	0.018	N/A				
	N,N-dimethyla cetamide		5 mL	0.063	0.32				
	MWCNT					42.35	24.49	-	7
carbon-based nanoadsorbent	SWCNT					676	24.29	-	8
	MWCNT, carboxylic acid					116.5	77	-	9
	functionalized Graphene oxide					2215	294	0.016 ($C_{Cu^{2+}, initial} = 10$ 5 mg L^{-1})	10
	Soy protein-based PEI hydrogel	soy protein isolate	1 g	0.06	0.06	1.78	136.2	0.0046 ($C_{Cu^{2+}, initial} = 11$ 100 mg L^{-1})	11
biomass-based adsorbent	PEI (Mw % ca. 25000)		1 g	1.72	1.72				
	epichloroh ydrin		N/A						
	soybean dregs-PAA	Soybean dregs	0.60 g	N/A		0.11	75.4	0.0333 ($C_{Cu^{2+}, initial} = 12$ 150 mg L^{-1})	12
	tea waste					N/A	48	0.0133 ($C_{Cu^{2+}, initial} = 13$ 200 mg L^{-1})	13
	Activated slag					N/A	30	-	14

Sewage sludge			N/A	83	-	15
CKS	soybean dregs	1 g	8.3×10^{-7}	8.3×10^{-7}	0.041	0.0002 ($C_{Cu^{2+}, initial} = 100 \text{ mg L}^{-1}$)
	CaSO ₄	1 g	0.022	0.022		This work
	oxalate	1 g	0.019	0.019		

Detailed information: CNC, cellulose nanocrystals; DNPH, 2,4-Dinitrophenylhydrazine; PEI, polyethylenimine; PAA, poly(acrylic acid)

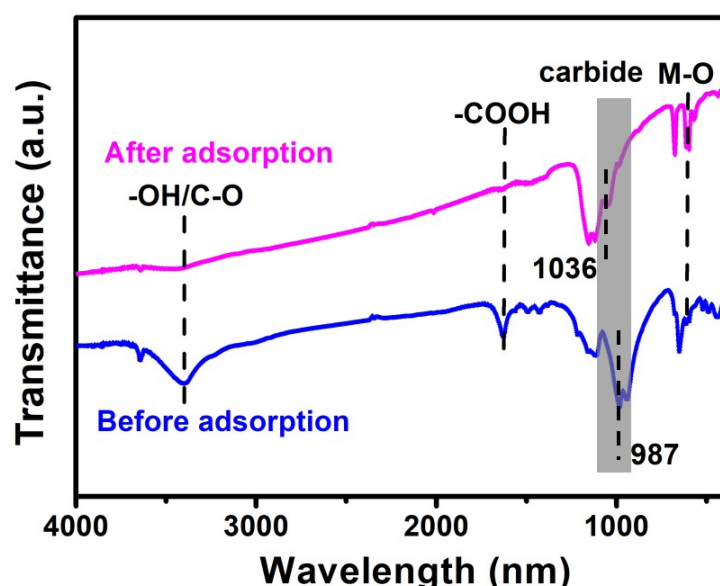


Figure S7. FT-IR spectra of CKS before and after Cu(II) adsorption.

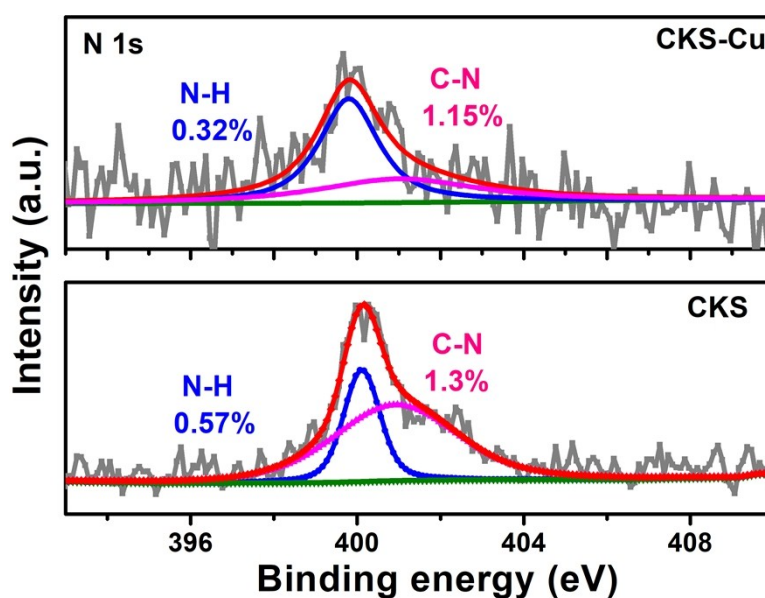


Figure S8. XPS detailed studies of N 1s signal deconvolution of CKS biosorbent before and after Cu²⁺ adsorption.

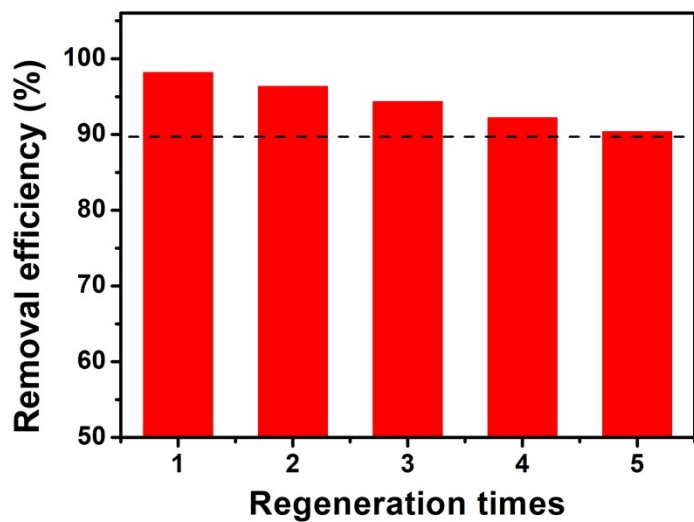


Figure S9. Cu(II) removal efficiency and recycling of CKS biomass adsorbents. The initial concentration of Cu(II) is 10 mg L⁻¹.

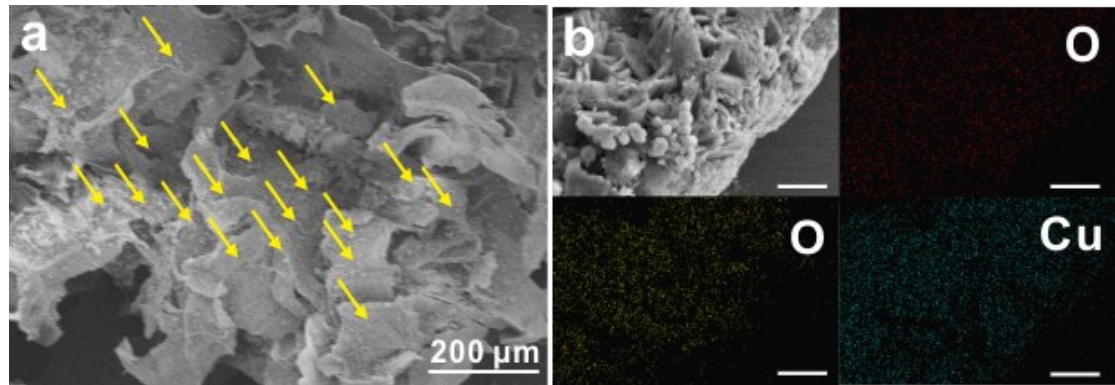


Figure S10. a) SEM image of CKS, the arrows label the Cu nanoparticles on the surface of CKS. b) Mapping images of CKS-Cu, the scale bar is 2 μm.

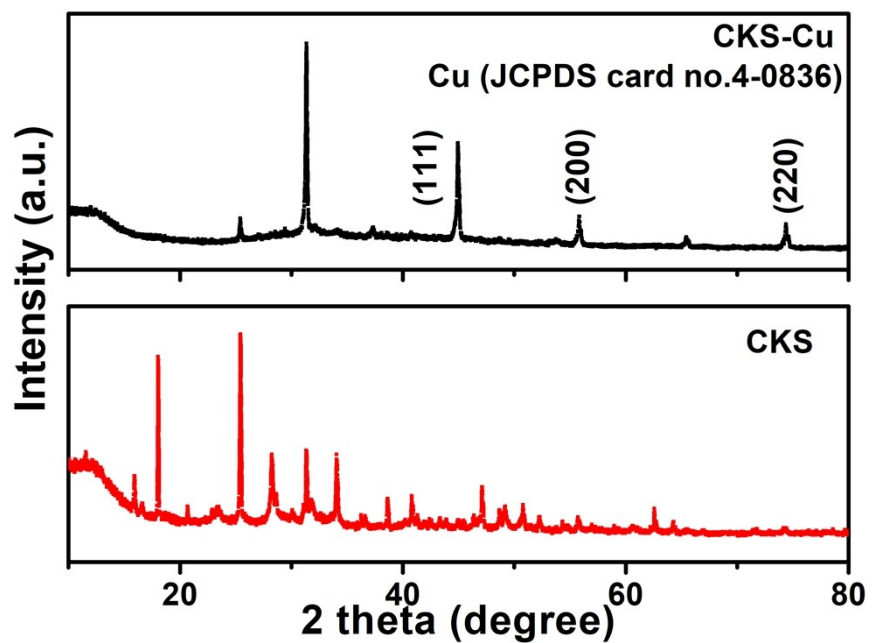


Figure. S11 XRD patterns of CKS before and after Cu^{2+} adsorption.

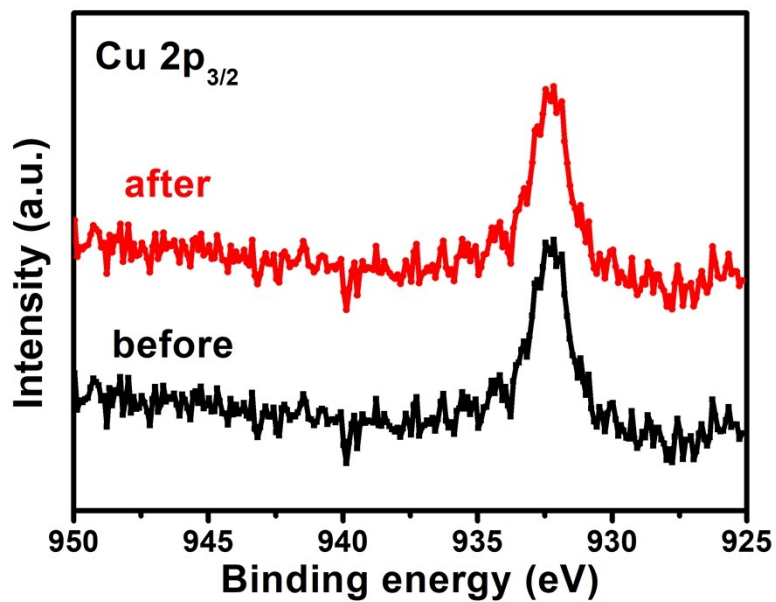


Figure. S12 XPS patterns of $\text{Cu} 2\text{p}$ of CKS-Cu before and after Cr^{VI} reduction.

Reference:

- [1] Y.-H. Chen, F.-A. Li, *J. Colloid Interface Sci.*, 2010, **347**, 277-281.
- [2] J. Hu, G. H. Chen, I. M. C. Lo, *Water Res.*, 2005, **39**, 4528-4536.

- [3] J. Pakarinen, R. Koivula, M. Laatikainen, K. Laatikainen, E. Paatero, R. Harjula, *J. Hazard. Mater.*, 2010, **180**, 234-240.
- [4] R. Koivulaa, J. Pakarinenb, M. Siveniusb, K. Sirolab, R. Harjulaa, E. Paaterob, *Sep. Purif. Technol.* 2009, **70**, 53-57.
- [5] W. Zhao, I. W. Chen, F. Xu, F. Huang, *J. Mater. Chem. A*, 2017, **5**, 15724-15729.
- [6] S. Hokkanen, A. Bhatnagar, M. Sillanpää, *Water Res.* 2016, **91**, 156-173.
- [7] Y. H. Li, J. Ding, Z. Luan, Z. Di, Y. Zhu, C. Xu, B. Wei, *Carbon*, 2003, **41**, 2787-2792.
- [8] O. Moradi, K. Zare, M. Monajjemi, M. Yari, H. Aghaie, *Fullerenes, Nanotubes, and Carbon Nanostructures*, 2010, **18**, 285-302.
- [9] J. Liu, D. Su, J. Yao, Y. Huang, Z. Shao, X. Chen, *J. Mater. Chem. A*, 2017, **5**, 4163-4171.
- [10] R. Sitko, E. Turek, B. Zawisza, E. Malicka, E. Talik, J. Heimann, R. Wrzalik, *Dalton Trans.*, 2013, **42**, 5682-5689.
- [11] J. Liu, D. Su, J. Yao, Y. Huang, Z. Shao, X. Chen, *J. Mater. Chem. A*, 2017, **5**, 4163-4171.
- [12] M. Zhang, L. Song, H. Jiang, S. Li, Y. Shao, J. Yang, J. Li, *J. Mater. Chem. A*, 2017, **5**, 3434-3446.
- [13] B. M. Amarasinghe, P. K., W., R. A. Williams, *Chem. Eng. J.*, 2007, **132**, 299-309.
- [14] V. K. Gupta, *Ind. Eng. Chem. Res.*, 1998, **37**, 192-202.
- [15] S. Rio, C. Faur-Brasquet, L. Le Coq, P. Courcoux, P. Le Cloirec, *Chemosphere*, 2005, **58**, 423-437.